

Shear and Compression Viscoelasticity in Polymer Monolayers

Toby A. M. Ferenczi † and Pietro Cicuta †§

† Cavendish Laboratory, University of Cambridge, Madingley Road, Cambridge Cb3 0HE, U.K.

Abstract. Poly-vinylacetate (PVAc) forms very stable and reproducible monolayers on the surface of water, a model system to understand polymer physics on two dimensions. A recently introduced technique is applied here to study viscoelasticity of PVAc monolayers. The method is based on measurement of surface tension in two orthogonal directions during anisotropic deformation. Compression and shear moduli are explored over a very large concentration range, highlighting a series of four different regimes. At low concentration the polymers are in a dilute gas. Above the overlap concentration Γ^* there is a fluid semi-dilute region, where the monolayer properties are described by scaling laws. At a threshold concentration Γ^{**} , a decrease in the gradient of pressure with concentration is observed, and we argue that there is still a large fraction of free area on the surface. Compressing further, we then identify close packing as the point where the pressure gradient rises sharply and a shear modulus emerges. This is interpreted as a transition to a soft-solid due to the kinetic arrest of close-packed monomers. The rheological properties of PVAc above Γ^{**} have not been studied previously. Discussion includes possible explanations for the observed behaviour in terms of both equilibrium and non-equilibrium conditions, and the relation to microscopic chain properties. Temperature dependent effects around Γ^{**} are also observed and described.

1. Introduction

Polymer physics has evolved over the last 50 years into a highly successful and sophisticated set of theories [1, 2]. A significant area of uncertainty remains in the application of some of these ideas to polymers confined to two dimensions (2D). This is partly due to the greater experimental challenge in establishing well controlled two dimensional systems. One approach is to spread polymers on the surface of a liquid, to form Langmuir films. Recent developments in surface rheometry [3, 4, 5, 6] are now enabling experiments that probe the viscoelastic properties of 2D polymer solutions as a function of concentration and frequency, in analogy with similar classical experiments in bulk solutions. Some three dimensional behavior has a direct correspondence in two dimensions, for example the existence of a semi-dilute

§ To whom correspondence should be addressed (pc245@cam.ac.uk)

concentration regime where the excluded volume effect is progressively screened [7]. Recent experiments indicate that other behavior, in particular relating to chain dynamics, is unique to two dimensions. For example for a large set of different monolayers the compressional dynamics is described by a timescale that is not related to the classical reptation mechanism [6].

In this work a very well studied system is chosen: monolayers of polyvinylacetate (PVAc) on the surface of water [7, 8, 9, 10, 4, 5]. The equilibrium and dynamical properties of this system are well known at low concentrations. In this work measurements are extended to very high concentration, where surprisingly we observe the development of a finite shear modulus. The presence of a glass transition at low temperatures has been suggested for PVAc layers [11] and this is also re-examined here.

2. Theoretical Background

2.1. Viscoelasticity of Monolayers

In a Langmuir trough experiment the surface tension is measured as a function of available surface area. For an insoluble monolayer the surface concentration is related inversely to the area A , $\Gamma = M/A$, where M is the mass on the surface. Surface pressure is identified as the resultant drop in surface tension as concentration increases, from the value γ_0 of the clean interface, $\Pi_{eq} = \gamma_0 - \gamma$.

In general, the response to an arbitrary deformation can be characterised by two independent moduli: compression, ε and shear, G . For isotropic and quasi-static compressions the ‘equilibrium modulus’ ε_{eq} is probed, whereas at finite compression strain rates, a viscosity η_d would be observed. ε_{eq} is an elastic (storage) component proportional to the derivative of pressure with area, and η_d is due to dissipation from frictional resistance to the flow:

$$\varepsilon_{eq} = \Gamma \left(\frac{\partial \Pi_{eq}}{\partial \Gamma} \right)_T \quad \text{and} \quad \eta_d = A \frac{\Pi - \Pi_{eq}}{\frac{d}{dt} A}. \quad (1)$$

The complex shear modulus is defined as the ratio of shear stress response to an induced strain (at constant area). As usual in linear viscoelasticity, the complex dynamic moduli for compression (ε^*) or shear (G^*) can be measured following oscillatory deformations,

$$\varepsilon^*(\omega) = \varepsilon'(\omega) + i\varepsilon''(\omega); \quad G^*(\omega) = G'(\omega) + iG''(\omega), \quad (2)$$

where ω is the frequency of oscillation and $\varepsilon''(\omega) = \omega\eta_d(\omega)$. In eq. 2 the real and imaginary parts describe the in-phase (elastic) and the out of phase (dissipative) components of the response.

As recently described in [12], it is possible in surface monolayers to determine both ε^* and G^* from the full stress response $\Pi(t)$. This is because under uniaxial compression of a Langmuir film *both* compression and shear deformation are exerted, although contribution from shear is often small and treated as negligible. Petkov

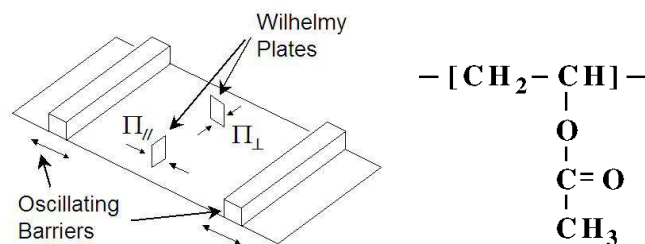


Figure 1. (a) Schematic diagram of Langmuir trough setup for anisotropic measurements of surface pressure. (b) Chemical diagram of vinyl acetate monomer [14].

et al. [13] were the first to show a directional anisotropy in surface pressure measurements using two Wilhelmy plates arranged in orthogonal directions, see Fig. 1. This anisotropy is directly dependent on the shear modulus. It was shown that for sinusoidal deformations of the form $\delta A(t)/A_0 = \Delta A/A_0 \cos \omega t$, the pressure response can be expressed as

$$\begin{aligned} \Pi_{\parallel} - \Pi_0 &= \delta \Pi_{\parallel}(t) = \frac{\Delta A}{A_0} [(\varepsilon' + G') \cos \omega t + (\varepsilon'' + G'') \sin \omega t] \\ \Pi_{\perp} - \Pi_0 &= \delta \Pi_{\perp}(t) = \frac{\Delta A}{A_0} [(\varepsilon' - G') \cos \omega t + (\varepsilon'' - G'') \sin \omega t]. \end{aligned} \quad (3)$$

2.2. Concentration regimes for polymers in monolayers

Although the separation of concentration into three regions (dilute, semi-dilute and concentrated) has been proposed before, it is worth summarizing here some of the key ideas, because they underpin the discussion of the different dynamical response regimes studied in this paper. For isolated polymer chains the mean end-to-end distance is well known, $R \simeq aN^{\nu}$, given that ν is the Flory exponent [15], a is the monomer size and N the number of monomers per chain. This expression for R would be an equality if a were replaced by the statistical Kuhn length b , and N by aN/b . For very flexible polymers like PVAc the two lengths a and b are likely to be very similar. In the case of two dimensions and for excluded volume type interactions, theoretical predictions for neutral polymers give $\nu = 0.75$ [1, 7]. Such a chain is said to be in ‘good’ solvent conditions and obeys a self avoiding walk conformation.

If the average separation between chains is greater than R the system can be thought of as a two dimensional gas, resulting in a linear relation between surface pressure and surface concentration. Chains are no longer isolated above the overlap concentration, Γ^* , defined as the concentration where overall surface concentration is the same as that within each unperturbed chain. The dependence of Γ^* on N follows from this definition,

$$\Gamma^* \sim \frac{N \text{ [monomer mass]}}{R^2} \sim N^{(1-2\nu)}. \quad (4)$$

The behaviour above Γ^* is known as the semi-dilute regime and detailed description may be found in refs. [1, 2]. Briefly, the presence of surrounding chains results in the progressive screening of intra-chain repulsive interactions, until eventually at high monomer density (a melt) the behaviour of the chain becomes ideal. A characteristic length, ξ , can be introduced: below ξ the chain does not interact with other chains and thus still obeys a self avoiding walk; above ξ the chain can be seen as a succession of ‘blobs’ following an ideal random walk. At Γ^* , $\xi \sim R$ and, as the chains are compressed, the characteristic length decreases rapidly. Scaling laws are obtained for the equilibrium pressure and compression modulus of a polymer film by assuming that the equilibrium properties in the semi-dilute regime only depend on ξ and not on N :

$$\Pi_{eq} \simeq \frac{k_B T}{R^2} \left(\frac{\Gamma}{\Gamma^*} \right)^{y_{eq}} \quad \text{and} \quad \varepsilon_{eq} = y_{eq} \Pi_{eq}, \quad \text{with} \quad y_{eq} = \frac{2\nu}{(2\nu - 1)}. \quad (5)$$

Polymer monolayers in the semidilute regime are fluid, and have negligible shear elasticity and viscosity. Their compressional dynamics has been the focus of recent investigations that have shown scaling of the compressional viscosity [6], a particularly surprising result because it indicates a relaxation mechanism specific to two dimensional layers.

The semidilute regime ends at a concentration Γ^{**} when the correlation length ξ becomes of the order of the monomer size. To be more precise in defining Γ^{**} , the distinction should be made between three lengths: the monomer size a , the statistical length (Kuhn length) b , and R_{sw} . The distinction between a and b also matters in determining exactly Γ^* , and was introduced above. The length scale R_{sw} becomes relevant if there are repulsive interactions between monomers described in terms of a Flory-type positive second-virial coefficient, v_2 [2, 16]. Then it is found that swollen behaviour (i.e. $R \sim N^{0.75}$) is only realised above a minimal monomer number N_{sw} , below which chain statistics are unaffected by the interaction. R_{sw} is expected to be of the order of a few segment lengths a [16]. The semi-dilute regime will end when the ‘characteristic length’ ξ reduces to the largest of the length scales discussed here, that is R_{sw} . At that point the entire system becomes statistically ideal. There are currently no experiments to distinguish precisely which of a , b or R_{sw} are limiting the semidilute regime, and different polymers may not be limited by the same length. The key point in considering Γ^{**} is that the area fraction Φ^{**} actually covered by monomers at this concentration can be quite low, somewhere between 20% to 35%. These very rough estimates are based either on R_{sw} being between $2a$ and $3a$, or considering that ξ reduces all the way down to a , but observing that the monomer area is roughly $a^2/3$ which is plausible given the monomer structure, see fig. 1(b). Measurements discussed below of the ratio Γ^{**}/Γ^* support this estimate.

3. Experimental Methods

Experimental methods are very similar to those described in [12] for measurements on protein layers, so only the most important facts are summarized here. The monolayer is contained within a Langmuir trough of total area 530cm^2 and width 20cm with two symmetrical barriers (mod. 610, Nima Technology, UK). Surface pressures Π_{\parallel} and Π_{\perp} are determined using two filter paper Wilhelmy plates, positioned at the center of the trough, one parallel and the other perpendicular to the compression direction. Polymer solution, typically $60\mu\text{l}$ of a 0.1mg/ml solution in tetrahydrofuran (analytical grade, Fisher Scientific) is spread onto an ultrapure water subphase in a dropwise fashion using a microsyringe. After spreading, the layer is left for at least 30 minutes to allow the solvent to evaporate and for the layer to reach equilibrium. The PVAc used throughout this investigation has molecular weight $M_w = 170,000\text{g/mol}$ (Acros organics), except for one experiment reported below where $M_w = 17,000\text{g/mol}$ is used (American Polymer Standards Corporation). Temperature of the subphase is controlled via water circulating under the trough.

To measure viscoelasticity the area is changed by oscillatory motion of the barriers, keeping the fractional amplitude of oscillation constant at $\Delta A/A_0 \sim 2\%$. The surface pressure response is recorded as a function of time by both Wilhelmy plates. Maximum accuracy is achieved by using the same sensor, and repeating each experiment spreading identical layers with the sensor's plate in each orientation. This is done at low concentrations, where any viscous effect is expected to be small. Two different sensors are used simultaneously as depicted in fig. 1 when the effect of the compressional viscosity and shear modulus are very large, as at high concentrations (Fig. 4). Data is collected every 0.1s , and about ten oscillations are made at each pressure, at two barrier speeds corresponding to periods of roughly 10s and 24s . Consideration of the propagation time of compression waves must be taken into account, as described in ref. [12].

4. Results and discussion

4.1. Dilute to Semi-Dilute and Concentrated regimes

Figures 2(a) and 2(b) are isotherms showing equilibrium surface pressure Π_{eq} and compression modulus ε_{eq} . The curves are independent of the orientation of the Wilhelmy plates. There is a power-law region extending up to $\Gamma^{**} = 0.75\text{mg/m}^2$, where the exponent $y_{eq} = 2.8 \pm 0.2$, corresponding to a Flory exponent of $\nu = 0.78 \pm 0.03$. This is in agreement with 'good' solvent predictions and other studies of PVAc [11, 10, 7, 5, 6]. The only direct indication of the point of overlap is the change in slope from 1 to y_{eq} in a logarithmic plot of surface pressure with concentration. For high molecular weight $M_w = 170000$, $N = 1977$ and the dilute regime ends at a very low concentration. Therefore the linear relation between pressure

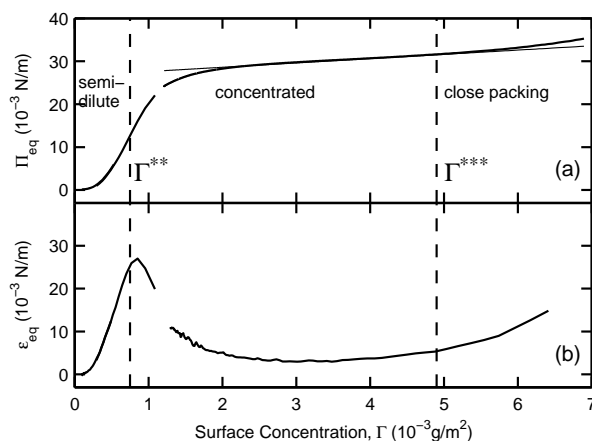


Figure 2. (a) Surface pressure, Π_{eq} and (b) equilibrium compression modulus ε_{eq} as a function of surface concentration over the entire concentration range at 6°C . The straight line interpolating the data between 2 and $5\text{mg}/\text{m}^2$ has a gradient of 1. The vertical lines identify the end of the semi-dilute regime and the deviation from a linear gradient in the pressure.

and concentration is at very low pressures, below the experimental resolution, in agreement with [7]. Isotherm measurements with a much lower molecular weight $M_w = 17000$ ($N \simeq 200$) (not shown) do display a clear dilute-semidilute transition, at $\Gamma_{17000}^* = 0.17 \pm 0.01\text{mg}/\text{m}^2$ and $\Pi_{17000}^* = 0.45 \pm 0.02\text{mN}/\text{m}$. This is in good agreement with the value of $\Gamma_{17000}^* = 0.19$ that is obtained using eq. 4 and estimating R from the known bond length of $a = 0.23\text{nm}$ [14]. However these measurements of Γ^* are very delicate, because of the very low pressures involved and in particular the very high compressibility of the gas phase, that causes extremely long equilibration times (even hours) for the concentration across the surface. Indeed, the same overlap values as seen for $M_w = 17000$ have been reported recently for $M_w = 90000$ [5]. An uncontroversial determination of Γ^* can only come from measurements on a series of molecular weights. For $M_w = 17000$ a value of $\Gamma = 0.80$ is obtained for the peak position of the dilational modulus, the same as in Figure 2(b). This means that the $M_w = 17000$ layer has been compressed by a factor of around 4 between Γ^* and Γ^{**} . The packing fraction Φ of monomers can be estimated assuming each monomer occupies an area a^2 . Then the packing fraction for $M_w = 17000$ at Γ^* is $\Phi^* \simeq 0.07$, and at Γ^{**} $\Phi^{**} \simeq 0.28$. This confirms the previous argument on the possibility of considerable free space at Γ^{**} .

Above Γ^{**} , Figure 2(a) shows an interesting linear dependence of the surface pressure on the concentration. In this regime, that we call concentrated, the concentration increases by a factor of roughly 6 from $0.75\text{mg}/\text{m}^2$ to $4.8\text{mg}/\text{m}^2$. The linear pressure dependence could be due to the entropic cost of compressing what is essentially a gas of monomers rather than swollen regions. This picture assumes that the system remains in equilibrium throughout. Further investigation of the pressure divergence as the area per monomer decreases are needed to check this hypothesis.

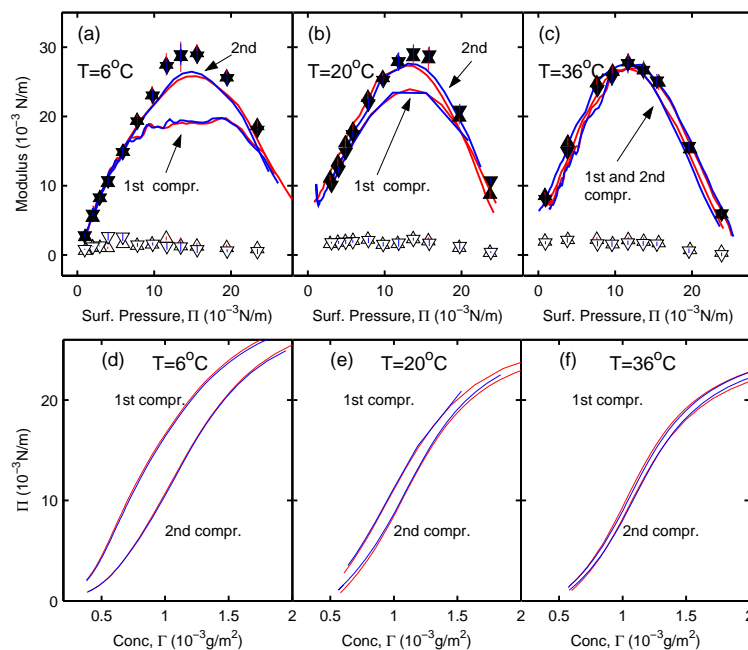


Figure 3. In (a), (b) and (c) lines are ε_{eq} recorded in perpendicular orientations, at different temperatures. Differences between first and second compressions are very marked at low temperature. Symbols correspond to measurements of dynamic moduli: (\blacktriangle) $\varepsilon' + G'$, (\blacktriangledown) $\varepsilon' - G'$, (\triangle) $\varepsilon'' + G''$ and (\triangledown) $\varepsilon'' - G''$. The concentration loss effect described in the text between first and second compression isotherms is shown in (d), (e) and (f). Π_{\parallel} and Π_{\perp} are indistinguishable in this range.

4.2. Temperature effects

The measurements in figures 3(a), (b) and (c) correspond to the semi-dilute and beginning of the concentrated regimes. A surprising result is that at low temperatures the first compression isotherm differs from a second compression exerted after re-expansion of the same monolayer. Further compressions are identical to the second. This effect is most evident at the lowest temperature. Looking at figure 3(d) it would appear that there has been a loss of concentration after the first compression. We think that at low temperatures some of the polymer conformations with long timescales become frozen out due to steric or ‘jamming’ effects. The system then enters a regime where only short timescale configurations are taking place which causes a reduction in the free energy cost of compression, leading to the observed drop in pressure gradient. Upon re-expansion these conformations remain ‘frozen’, thus reducing the effective density of the layer. The experiment reported here seems another manifestation of the temperature dependence of the thermal expansion coefficient reported in [11]. Note that for compressions after the first, the semi-dilute regime shows very similar behavior at all temperatures. In all experiments in this concentration range $\varepsilon' + G'$ and $\varepsilon' - G'$ are the same, which implies close to zero shear elasticity in the semidilute region. Well below Γ^{**} ε' and ε_{eq} are indistinguishable. Close to Γ^{**} the complex compressional

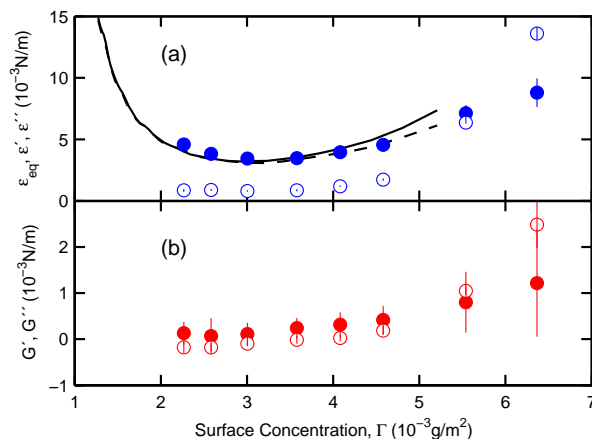


Figure 4. (a) Compression and (b) Shear moduli concentration, at very high concentration and $T=6^\circ\text{C}$. Solid and dashed lines show ε_{eq} in parallel and perpendicular orientations respectively. Solid and empty symbols are the elastic and viscous components.

elasticity, ε' becomes consistently greater than its equilibrium counterpart, ε_{eq} . The compression dynamic modulus remains in the power law regime until slightly higher pressures, which may be due to the small dynamical excitations allowing the polymers to explore more chain configurations (as described in [12]). The complex viscosities are finite but small (G'' always $\leq 2\text{mN/m}$) at this frequency and in this concentration range. Recent studies of PVAc Langmuir films [5, 6] have independently shown and explained with two different models the presence of scaling laws for compressional viscosity where the exponent is twice that for compressional elasticity, i.e. $\varepsilon'' \sim \Gamma^{2y_{eq}}$. This implies that compressional viscosity should follow a quadratic function of pressure, but the data presented here is unable to resolve this trend.

4.3. Close Packing

The linear dependence of pressure on concentration, as shown by the dashed line of fig. 2(a), lasts up to a concentration $\Gamma^{***} = 4.8\text{mg/m}^2$. We think that this concentration is very close to close packing of monomers on the monolayer. Even higher values (not shown here) of the pressure can be reached, however they are not stable over time. 30 hours after a compression to $\Pi \simeq 36\text{mN/m}$, the pressure had equilibrated to around 31.6mN/m , the value at Γ^{***} . Figure 4 shows that below $\Gamma = 3\text{mg/m}^2$ the shear modulus, G' remains zero and the equilibrium elastic modulus ε_{eq} is indistinguishable from the dynamic compressional modulus ε' . At a critical concentration, ε' increases sharply with pressure and eventually exceeds ε_{eq} . The viscous modulus ε'' also increases sharply after $\Gamma = 4\text{mg/m}^2$ and becomes greater than the elastic component. Both G' and G'' become non-zero approaching close packing, although neither becomes as large as the compressional components. We

further remark that the viscous shear component exceeds the elastic component at high concentration. Detailed analysis of these trends is premature.

It is probable that the shear modulus approaching close packing arises by a process of dynamical arrest due to crowding rather than by formation of a network structure. It has been shown from both simulation [17] and experiment [18] that systems of colloidal monolayers undergo kinematic arrest at surface fractions of $\Phi \simeq 0.8$. The effect is essentially caused by the caging of a particle by its neighbours due to hard core repulsion interactions. At high surface fractions, the behaviour of vinyl acetate monomers may be dominated by their hard core interactions as in colloidal systems. Some simulations have suggested that two dimensional systems of polymer chains may form interpenetrated, entangled networks at high concentration [19] whereas several other simulations [20] and experiments [21] have pointed out that chains confined to two dimensions remain as segregated disks, as also suggested in [1]. Our results appear to support the latter case because it is unlikely that solid behaviour would emerge only at $\Phi \sim 1$ if it was due entanglements.

The instability in the layer above Γ^{***} indicates that there is likely to be some collapse into the subphase at this concentration, but because such an effect is observed only at extreme concentrations we do not consider it necessary to explain the observed behavior at lower concentrations in terms of out-of-plane polymer rearrangement or multilayer formation.

5. Conclusions

The set of experiments reported here characterize the viscoelastic properties of poly(vinyl-acetate) monolayers over a concentration range of several orders of magnitude. Within this range we have identified four types of behaviour. Specifically, these are the dilute, semi-dilute, concentrated and close-packed regimes, separated by the transition concentrations, Γ^* , Γ^{**} and Γ^{***} . The dilute and semi-dilute regimes have previously been well defined and our results are in agreement with these descriptions. At higher concentration, the behaviour has been subject to far less scrutiny, due in part to experimental limitations. We have observed a region of linear pressure gradient that we argue is caused by the entropic cost of compressing a gas of monomers. This is followed by a region of close-packed behaviour resulting in the formation of a soft-solid, as evidenced by the emergence of a shear modulus. Temperature dependence of the compression modulus has been observed and interpreted as evidence of non-equilibrium effects. Using existing polymer theory the importance of microscopic length scales associated with the polymer chain has been stressed. This implies a degree of universality in the description of neutral homopolymers which presents interesting opportunities for further study.

Acknowledgments

P.C. thanks the Oppenheimer Fund for financial support.

- [1] P.-G. de Gennes. *Scaling Concepts in Polymer Physics*. Cornell University Press, Ithaca, 1979.
- [2] M. Doi and S. F. Edwards. *The Theory of Polymer Dynamics*. Oxford University Press, New York, 1986.
- [3] C. F. Brooks, G. G. Fuller, C. W. Curtis, and C. R. Robertson. *Langmuir*, 15:2450, 1999.
- [4] F. Monroy, F. Ortega, and R. G. Rubio. *Phys. Rev. E*, 58:7629, 1998.
- [5] F. Monroy, H.M.Hilles, F. Ortega, and R. G. Rubio. *Phys. Rev. Lett.*, 91:268302, 2003.
- [6] P. Cicuta and I. Hopkinson. *Europhys. Lett.*, 68:65, 2004.
- [7] R. Vilanove and F. Rondelez. *Phys. Rev. Lett.*, 45:1502, 1980.
- [8] R. A. L. Jones and R. W. Richards. *Polymers at Surfaces and Interfaces*. Cambridge Univ. Press, Cambridge (U.K.), 1999.
- [9] K.-H. Yoo and H. Yu. *Macromolecules*, 22:4019, 1989.
- [10] B. B. Sauer, H. Yu, M Yazdanian, G Zograf, and M.W. Kim. *Macromolecules*, 22:2332, 1989.
- [11] F. Monroy, F. Ortega, and R. G. Rubio. *Eur. Phys. J. B*, 13:745, 2000.
- [12] P. Cicuta and E.M. Terentjev. *European Phys. J. E*, 16:147, 2005.
- [13] J. T. Petkov, T. D. Gurkov, B. E. Campbell, and R. P. Borwankar. *Langmuir*, 16:3703, 2000.
- [14] In J. Bandrup, E. H. Immergut, and E. A. Grulke, editors, *Polymer Handbook*, New York, 1999. Wiley.
- [15] P.J. Flory. *Principles of Polymer Chemistry*. Cornell University Press, Ithaca, 1953.
- [16] R. R. Netz and D. Andelman. *Physics Reports*, 380:1–95, 2003.
- [17] L. Santen and W. Krauth. *Nature*, 405:550, 2000.
- [18] P. Cicuta, E. J. Stancik, and G. G. Fuller. *Phys. Rev. Lett.*, 90:236101, 2003.
- [19] B. Ostrovsky, M. Smith, and Y. Bar-Yam. *Int. J. Mod. Phys. B*, 8:931, 1997.
- [20] I. Carmesin and K. Kremer. *J. Phys. France*, 51:915, 1990.
- [21] B. Maier and J. O. Rädler. *Phys. Rev. Lett.*, 82:1911, 1999.